A new model for ejected particle velocity from erupting bubbles in 2-D fluidized beds

J.A. Almendros-Ibáñez*, C. Sobrino, M. de Vega, D. Santana

Departamento de Ingeniería Térmica y de Fluidos, Universidad Carlos III de Madrid, Avda. de la Universidad 30, 28911 Leganés, Madrid, Spain

Abstract

A new model is proposed for obtaining the velocity profile of the particle ejected from the bubble dome in a freely bubbling 2-D fluidized bed. Its basis is the supposition that the initial velocity of the ejected particles, with a direction perpendicular to the dome contour, depends on bubble velocity and bubble growth velocity. This model differs from those previously appearing in the literature in that it is valid not only for vertical-ascent circular bubbles.

Experiments were carried out in a freely bubbling 2-D fluidized bed using a high-speed video camera to measure the velocity profile. Upon comparing these results with the proposed model, it was established that, excepting some isolated cases, the model properly predicts the magnitude and direction of the maximum particle ejection velocity and the velocity profile.

Using the work of Shen et al. (2004. Digital image analysis of hydrodynamics two-dimensional bubbling fluidized beds. Chemical Engineering Science 59, 2607–2617), we obtain two general equations for the bubble velocity and the bubble growth velocity in a 2-D fluidized bed. These expressions, together with the proposed model, can be used to calculate the initial velocity of the ejected particles.

Keywords: Fluidized bed; Erupting bubble; Particle ejection

1. Introduction

Fluidized beds are widely used in the industry as, among others, dryers, chemical reactors, biomass and coal combustors/gasifiers. They possess a high *reaction/volume* ratio due to high mixing and turbulence levels, thus creating a uniform temperature throughout the whole dense bed. For most of the industrial applications, the fluidized inert particles are group B, according with Geldart's classification (Geldart, 1973). With this type of particles, when the superficial gas velocity exceeds the minimum velocity for fluidization conditions, the excess gas traverses the dense bed in the form of bubbles.

Along their ascent, the bubbles undergo coalescence and ingest the surrounding air from the emulsion phase, thus causing them to grow. When a bubble erupts at the bed surface, it projects particles into the freeboard, although the particles' point of origin is unclear. Pemberton and Davidson (1986) proposed two ejection mechanisms: ejection from the bubble dome or ejection from the bubble wake. The former is predominant in the case of isolated erupting bubbles, while for high superficial gas velocities the wake mechanism becomes more important due to coalescence. In addition, the effect of the vessel walls is important because they mitigate wake ejection (Pemberton and Davidson, 1986), the result being a greater predominance of the dome mechanism in 2-D fluidized beds.

The projection of particles by the erupting bubbles into the freeboard is the main cause of their elutriation and/or entrainment (entrainment is defined as the total flux of solids leaving the bed, while elutriation refers to the separation of fines from a wide mix of particles). The mass of particles in the freeboard decreases exponentially from the bed surface up to the transport disengaging height (TDH), which is one of the most important parameters in fluidized bed design. Beyond the TDH, entrainment is nearly constant. Some empirical correlations can be found in the literature for estimating this height, but they are largely uncertain. To properly calculate the TDH, it is

* Corresponding author. Tel.: +34916248884; fax: +34916249430.
E-mail address: jalmendr@ing.uc3m.es (J.A. Almendros-Ibáñez).

necessary to understand the process being undergone below it, namely, the formation and disintegration of coherent structures like clusters, vortex or ghost bubbles, as well as the interaction between the particles and the gas turbulence (Pemberton and Davidson, 1984; Duursma et al., 2001; Solimene et al., 2004). These processes are influenced by bubble eruption, the projection and velocity of the ejected particles and the maximum height they reach.

In order to calculate the maximum height attained by the projected particles, some theories are proposed in the literature, based in the integration of the momentum equation for isolated or grouped particles (Do et al., 1972; Peters and Prybylowski, 1983; Demmich, 1984; Fung and Hamdullahpur, 1993) and based in the momentum transferred to the particles by the gas bubble (Pemberton and Davidson, 1986). Each of these theories requires the initial velocity of the ejected particles. For example, Peters and Prybylowski (1983) assumed a constant radial velocity normal to the dome contour, Demmich (1984) suggested that the initial particle velocity profile follows an exponential relationship and Fung and Hamdullahpur (1993) supposed a symmetric distribution, in which the magnitude of the velocity vectors decays linearly with the angle measured from the vertical direction. These three models proposed for the particle ejection velocity profile are only valid for vertical-ascent spherical bubbles (circular bubbles in 2-D fluidized beds) erupting isolated at the bed surface. They are obtained for single injected bubbles, and are difficult to extrapolate to erupting bubbles in a freely bubbling fluidized bed.

Therefore, we present a new model for the velocity profile of the particles ejected from the bubble dome in these circumstances. This model, since it is proposed for a freely bubbling 2-D fluidized bed, is valid not only for vertical-ascent circular bubbles, but rather for all ascending directions including different bubble sizes and dome contours. Therefore, without disregarding its use for simple cases with vertical-ascent and/or circular bubbles, the model calculates the initial velocity of the particle ejected into the freeboard of a fluidized bed in conditions similar to real ones.

A cold 2-D fluidized bed, similar to the one described by Santana et al. (2005), is used in the experiments. We took photographs with a high-speed video camera and measured the initial velocity of the particles projected from the dome. The model was contrasted with the experimental results, and showed substantial agreement. Then, using the results of Shen et al. (2004), we obtained two equations for bubble velocity and bubble growth velocity in a 2-D freely bubbling fluidized bed. These equations, together with the proposed model, allow for the calculation of the velocity profile of the ejected particles.

2. Theoretical model

Different models appear in the literature for obtaining the velocity profile of the particles ejected from bubble eruption, though all of them are limited to vertical-ascent spherical bubbles. The first model was proposed by Peters and Prybylowski (1983), who assumed a constant radial velocity for all the particles. However, Santana et al. (2005) showed in their experiments that the velocity of the particles projected from the center of the dome is higher than that of the particles located near the stagnation points; from this they established Fung's model (Fung and Hamdullahpur, 1993) as the most appropriated for their experimental conditions. Fung's model assumes that the magnitude of the radial particle ejection velocity decreases linearly with the angle θ, according to

$$U_p = \begin{cases} U_{p,\max}\left(\dfrac{\theta}{\frac{\pi}{2}}\right) & \text{if } 0 \leqslant \theta \leqslant \dfrac{\pi}{2}, \\ U_{p,\max}\left(\dfrac{\pi-\theta}{\frac{\pi}{2}}\right) & \text{if } \dfrac{\pi}{2} \leqslant \theta \leqslant \pi, \end{cases} \tag{1}$$

where $U_{p,\max}$ is the maximum particle ejection velocity and θ is the angle formed by the velocity vectors and the bed surface. For 3-D fluidized beds, this velocity is two times the bubble velocity U_b (Pemberton and Davidson, 1986; Fung and Hamdullahpur, 1993). However, this simple model does not take into account two facts: (a) the bubble may not rise vertically, thus the maximum particle velocity vector ($\overrightarrow{U}_{p,\max}$) can form an angle $\theta \neq \pi/2$ and (b) the stagnation points undergoing separation because of the bubble's growth as it bursts at the bed surface, thus making for a non-zero velocity.

The stagnation points are the separation points between the arc formed by the dome of the erupting bubble and the bed surface. These points can be defined as the inflection points of the curve formed by them.

Our model (valid for non-spherical bubbles and non-vertical-ascent directions) posits that the particle ejection velocity is the sum of two terms. The first term, $\overrightarrow{U}_{p,b}$, is related to the bubble velocity of the erupting bubble (measured as the displacement of the bubble's center of mass) and the second term, $\overrightarrow{U}_{p,g}$, concerns the bubble growth velocity, defined as

$$U_g = \frac{\partial R_{\text{eq}}}{\partial t} = \frac{1}{2}\frac{\partial D_{\text{eq}}}{\partial t}, \tag{2}$$

where D_{eq} is the equivalent diameter, defined as the diameter of the circle with the same bubble area.

We suppose that the maximum particle velocity vector related to the bubble velocity is equal to the bubble velocity vector ($\overrightarrow{U}_b$) and perpendicular to the dome contour. The magnitude of $\overrightarrow{U}_{p,b}$ decreases linearly with the angle θ toward the stagnation points, as put forth in Fung and Hamdullahpur (1993). Therefore, the first term of the model can be written as

$$U_{p,b} = \begin{cases} U_b\left(\dfrac{\theta-\theta_{\min}}{\theta_b-\theta_{\min}}\right) & \text{if } \theta_{\min} \leqslant \theta \leqslant \theta_b, \\ U_b\left(\dfrac{\theta-\theta_{\max}}{\theta_b-\theta_{\max}}\right) & \text{if } \theta_b \leqslant \theta \leqslant \theta_{\max}, \end{cases} \tag{3}$$

where θ_b is the angle formed by the bubble velocity vector and the bed surface and $\theta_{\min}$ and $\theta_{\max}$ are the minimum and maximum angles formed by the velocity vectors of the ejected particles, respectively (see Fig. 1). The direction of $\overrightarrow{U}_{p,b}$ is defined by θ.

In bubbling fluidized beds, the bubbles grow as they ascend, until they reach a maximum bubble height (Shen et al., 2004). When the bubble nose reaches the bed surface, a cavity of depth

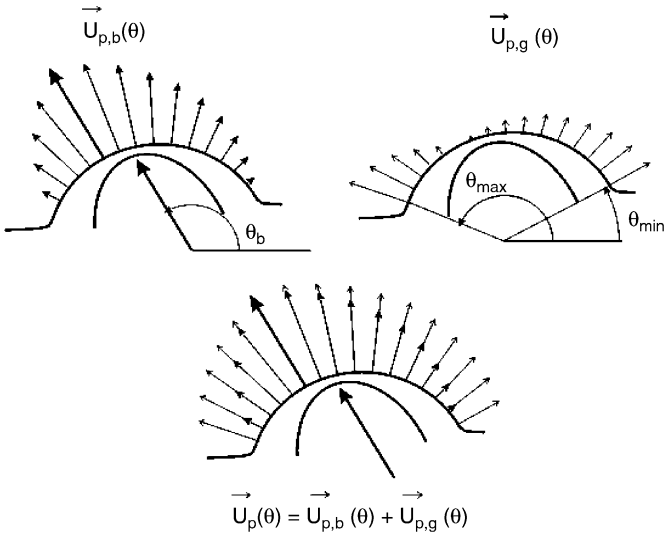

Fig. 1. Velocity profiles for $U_{p,b}(\theta)$ and $U_{p,g}(\theta)$. The sum of both is the particle ejection velocity $U_p(\theta)$.

equal to the bubble diameter is formed and the gas throughflow accelerates the particles in the bubble nose while the bubble breaks the bed surface (Glicksman and Yule, 1995). As the bubble rises, the depth of the cavity decreases and the gas flow through the bottom of the bubble is reduced. Then, the velocity of the gas crossing the dome also diminishes. Therefore, particles at the top of the bulge layer (Levy et al., 1982) decelerate due to the gravitational force become more important than the drag force, whereas in the stagnation points the gravitational force direction is practically perpendicular to the movement of such points. In consequence, the erupting bubble expands preferentially in the horizontal direction, i.e., the growth velocity is maximum at the stagnation points.

Levy et al. (1982) obtained implicitly similar results about the maximum growth velocity at the stagnation points. They showed that, as the bubble approaches to the bed surface, the distance between the top of the bulge layer and the top of the wake was coming close progressively. Therefore, as bubble's mass center approximates to the bed surface, the bubble form became more oblate.

Then, the bubble expands equally in all directions, but in its approach to the bed surface, the expansion is greater in the direction of the bed surface. When $\overrightarrow{U}_b$ has a horizontal component the erupting bubble tends to expand in the same direction. Hence, we assume that the maximum expansion velocities are reached at the stagnation points and $U_{p,g}$ decreases linearly until the point of maximum velocity $\overrightarrow{U}_{p,b}$. The direction of the particle ejection velocity due to the bubble growth is perpendicular to the dome contour, so it is defined by θ; and its magnitude is

$$U_{p,g} = \begin{cases} U_g(2 \pm \cos^2\theta_b)\left(1 - \dfrac{\theta - \theta_{\min}}{\theta_b - \theta_{\min}}\right) & \text{if } \theta_{\min} \leqslant \theta \leqslant \theta_b, \\ U_g(2 \mp \cos^2\theta_b)\left(1 - \dfrac{\theta - \theta_{\max}}{\theta_b - \theta_{\max}}\right) & \text{if } \theta_b \leqslant \theta \leqslant \theta_{\max}, \end{cases} \quad (4)$$

where the term $\cos^2(\theta_b)$ is added to the right side of the distribution ($\theta_{\min} \leqslant \theta \leqslant \theta_b$) when $\theta_b < \pi/2$ and vice versa. The term $2U_g$ takes into account that the growth velocity is maximum in the bed surface direction when the bubble erupts, and the term $U_g\cos^2(\theta_b)$ the effect of the non-vertical ascent of the bubble, that is, $\theta_b \neq \pi/2$. In this case, the bubble expands preferentially in the horizontal component of $\overrightarrow{U}_b$, as shown in Fig. 6(b) (where $\theta_b > \pi/2$) and the velocity on the left stagnation point is higher than the velocity on the right one.

Fig. 1 shows a sketch of both distributions.

In summary, the particle ejection velocity is the sum of both profiles (Eqs. (3) and (4)):

$$\overrightarrow{U}_p(\theta) = \overrightarrow{U}_{p,b}(\theta) + \overrightarrow{U}_{p,g}(\theta), \quad (5)$$

where the direction of the vector $\overrightarrow{U}_p$ is defined by θ.

It is important to note that the distribution of the particle ejection velocity is not symmetric unless the bubble ascends vertically, that is $\theta_b = \pi/2$ and $\theta_{\min}$ and $\theta_{\max}$ are supplementary ($\theta_{\min} = \pi - \theta_{\max}$). The velocity vectors are always normal to the dome, so the values of $\theta_{\min}$ and $\theta_{\max}$ are fixed by the dome's geometry, which depends on bubble shape and its interaction with surrounding bubbles.

In order to compare the proposed model with Fung's model, we can plot both profiles within one particular case of a vertical-ascent circular bubble bursting at the bed surface. The profiles of the non-dimensional velocity $U_p^* = U_p/U_{p,\max}$ are plotted in Fig. 2, and they show how Fung's model underestimates the horizontal component of the particle ejection velocity (Santana et al., 2005), while the differences in the vertical component are negligible, despite the fact that this only occurs for vertical-ascent circular bubbles. As shown in the experiments carried out by Santana et al. (2005), these differences are more pronounced in non-circular and non-vertical-ascent bubbles. Our work corroborates their results.

We have obtained the bubble velocity and the bubble growth velocity in 2-D fluidized beds, based on the work of

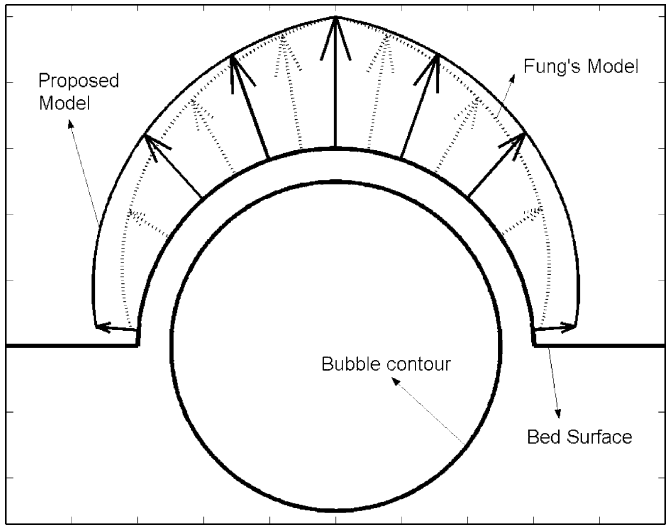

Fig. 2. Non-dimensional velocity profiles for a vertical-ascent circular bubble. Solid lines: proposed model, dotted lines: Fung's model. $D_b = 5\,\text{cm}$, $U_b = 57.5\,\text{cm/s}$ and $U_g = 8\,\text{cm/s}$.

Shen et al. (2004), who using an approach similar to the one used by Darton et al. (1977), obtained two expressions: one for bubble diameter and one for bubble velocity, both of which as a function of the height of the bed

$$D_b = \left(\frac{8(2^{3/4}-1)}{\lambda}\right)^{2/3} \times \left[(U-U_{mf})\left(h+\frac{\lambda}{\pi(2^{3/4}-1)}\frac{A_0}{b}\right)\right]^{2/3} g^{-1/3}, \quad (6)$$

$$U_b = \phi\sqrt{g\,D_b}, \quad (7)$$

where A_0 is the area of distributor divided by the number of orifices, b the bed thickness, h the height measured from the distributor, U_{mf} the minimum fluidization velocity, U the superficial gas velocity and λ and ϕ being constants to be determined experimentally. In their experiments they obtained $\lambda \sim 6.5$ and $\phi = [0.8–1.0]$.

On the other hand, the bubble growth velocity can be obtained as

$$U_g = \frac{1}{2}\frac{\partial D_b}{\partial t} = \frac{1}{2}\frac{\partial h}{\partial t}\frac{\partial D_b}{\partial h} = \frac{1}{2}U_b\frac{\partial D_b}{\partial h} \quad (8)$$

and introducing Eqs. (6) and (7) into Eq. (8), we obtain an expression for the bubble growth velocity as

$$U_g = \frac{1}{3}\left(\frac{8(2^{3/4}-1)}{\lambda}\right)\phi(U-U_{mf}). \quad (9)$$

Then, using Eqs. (3)–(5) together with the bubble velocity (Eq. (7)) and the bubble growth velocity (Eq. (9)), we can obtain the particle velocity profiles along the bubble dome contour of an erupting bubble at the bed surface.

3. Experiments

The experimental facility is shown in Fig. 3. A cold 2-D fluidized bed ($110 \times 60 \times 0.5$) cm was constructed. The compressed air was introduced into the plenum, 30 cm high, through two orifices situated on opposite sides of each other, thus ensuring the correct distribution of the flow. The distributor was a perforated plate with 110 holes 1 mm in diameter with a 1 cm gap between each. Both walls were made of glass, making it possible to see the bed and take photographs during the experiments.

The fluidized white-glass spherical particles had diameters ranging from 300 to 400 μm and a density $\rho_p = 2500\,\mathrm{kg/m^3}$. The minimum fluidization velocity was 0.6 m/s in all the experiments and the static bed height was approximately 25 cm. Experiments at different superficial gas velocities ($U/U_{mf} = 2, 3$ and 4) were carried out. For all the experimental conditions, the superficial gas velocity was lower than the terminal velocity of the smallest particles, making entrainment negligible.

The 2-D fluidized bed was illuminated with two 600-W spotlights situated at its front. A black card was placed at the rear, in order to create the maximum contrast between the emulsion phase (since the particles were white) and the bubble phase. The high-speed video camera shot 250 photographs per second with a resolution of 480 × 512 pixels. The images were analyzed following the process developed by Shen et al. (2004). The gray scale image was converted into a binary one using a threshold value, hence the bubble phase and the freeboard were transformed into white color and the emulsion phase into black. Then, the nearest bubble to the freeboard was selected and followed until its eruption at the bed surface. We fixed the eruption instant (see Fig. 4) for the moment in which the interior of the bubble entered into contact with the freeboard and there were no particles (black-colored objects in the

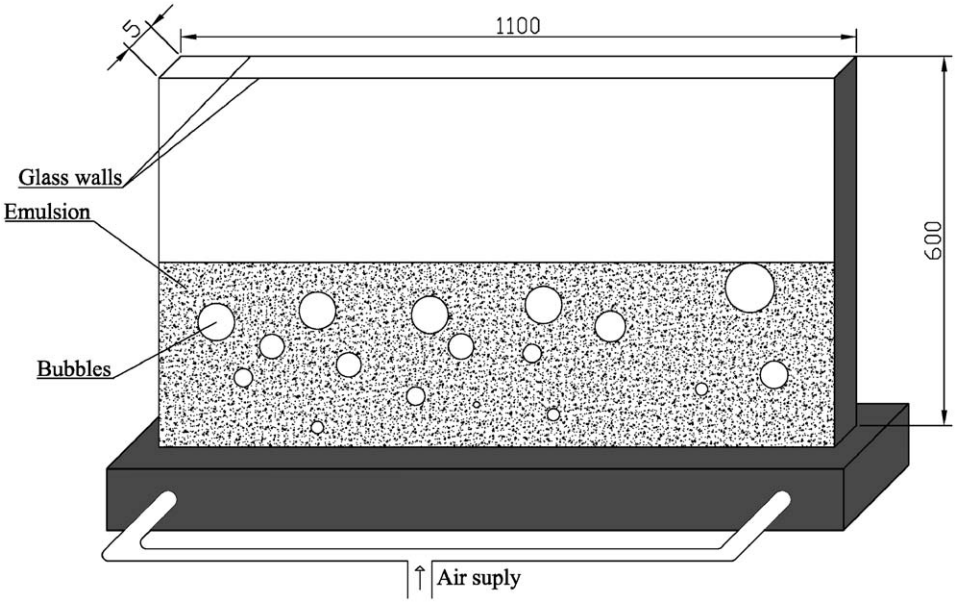

Fig. 3. Experimental layout. Dimensions in millimeters.

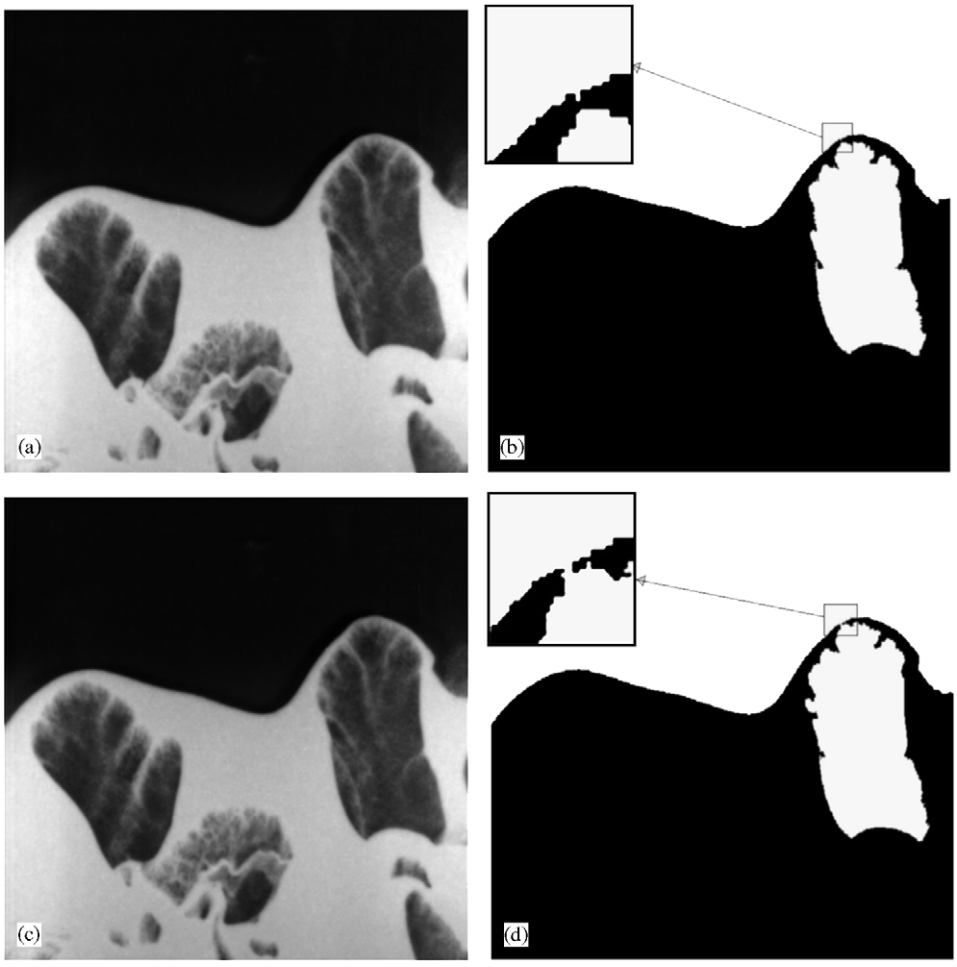

Fig. 4. Determination of the eruption instant: (a) and (c) original photographs (elapsed time: 4 ms), (b) and (d) treated photographs with a zoom in the breaking region.

photographs) between the freeboard and the bubble (Santana et al., 2005). Fig. 4 shows how in case (b) the bubble roof does not break the surface of the bed, while in the next photograph (0.004 s later) the bubble and the freeboard are joined.

For the last two frames before bubble eruption, we measured the bubble velocity, the bubble area and the bubble area equivalent diameter. With these last two frames, we were able to calculate the velocity profile of the ejected particles, which is perpendicular to the dome contour as Santana et al. (2005) showed in their experiments using a PIV technique. Fig. 5 explains the process for measuring particle ejection velocity by way of the example of the bursting bubble which appears in Fig. 4. First, we fit an ellipse to the contour of the dome in both photographs using a minimum-squared technique. Then, we traced the perpendicular line to the ellipse of the first photograph at each point. These lines intersect the dome contour of the second photograph. The length of the lines between the contours of both domes is the displacement of the particles ejected into the freeboard. With the time delay between frames (4 ms) we were able to calculate the velocity profile of the dome at the instant of eruption.

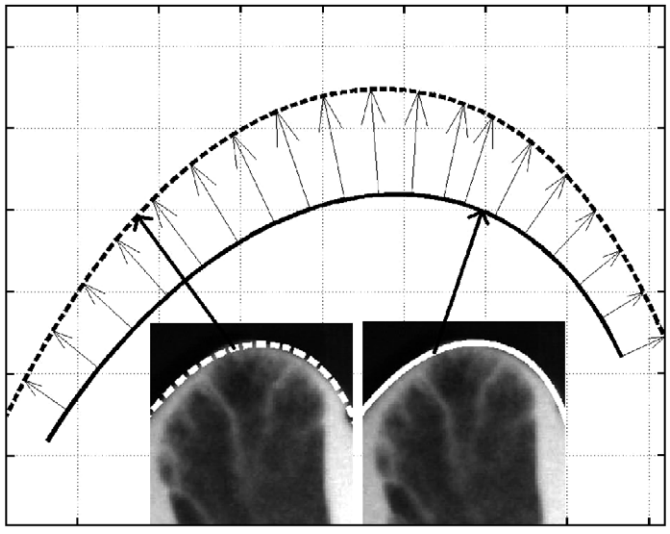

Fig. 5. Ellipses fitted to the dome contour of the two consecutive frames shown in Fig. 4(a), with a continuous line and (c), with a dotted line. The separation between both ellipses determines the dome velocity profile.

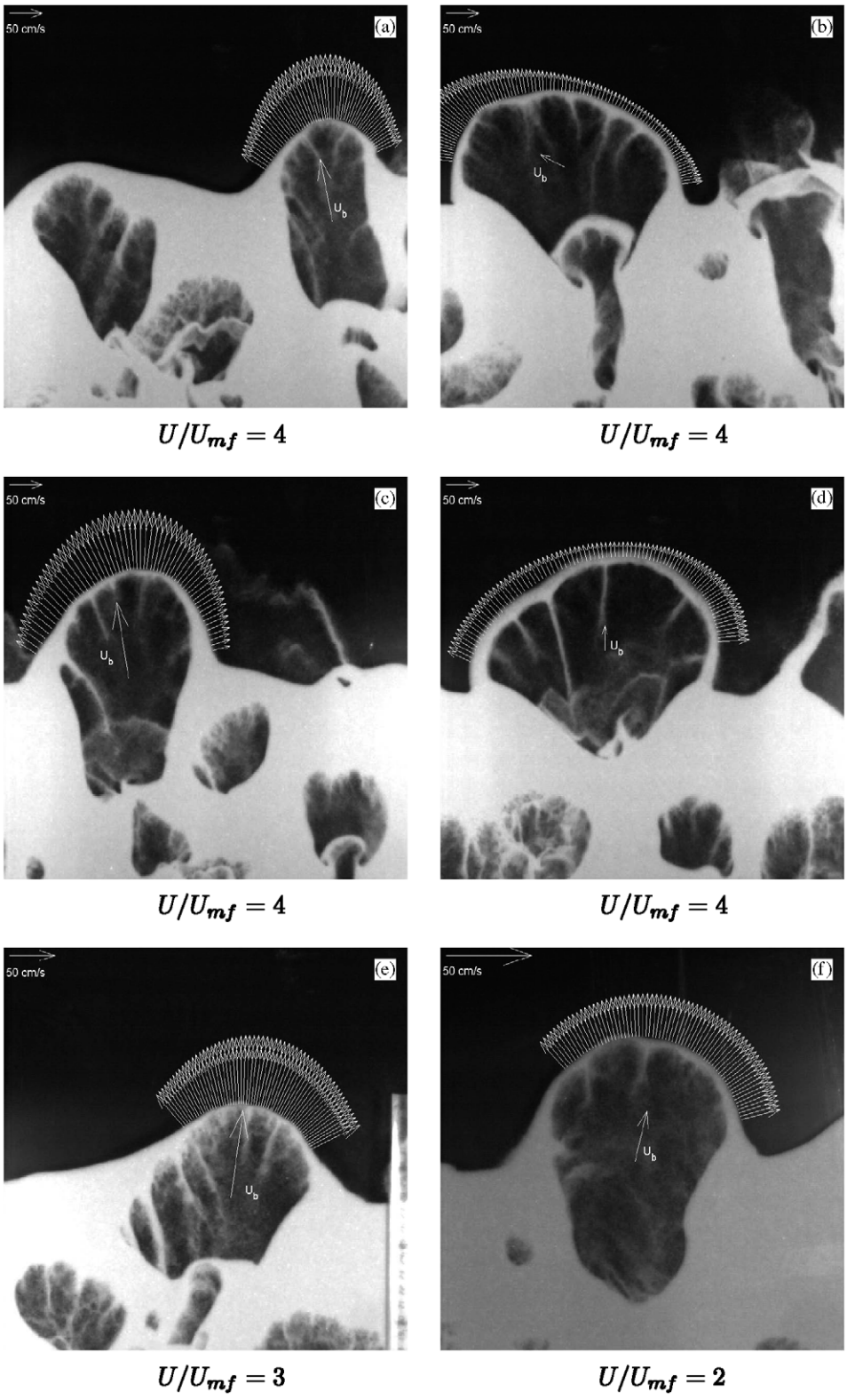

Fig. 6. Some examples of bubble eruption at different superficial gas velocities. Note that the scale of pictures (e) and (f) are different from the others. (d) shows a dome collapsed bubble.

4. Results and discussion

Different experiments have been carried out by varying the superficial gas velocity ($U/U_{mf} = 2$, 3 and 4). Since we used a freely bubbling fluidized bed in our experiments, the results obtained show a wide range of erupting bubbles, with different directions of ascent as well as bubble sizes, shapes and velocities. The bubbles followed the path forged by the

leading bubbles due to a more favorable pressure gradient. At the same instant, the neighboring bubbles disturb the bed surface when they burst. In all the experiments the height of the bed was below the maximum bubble height (Shen et al., 2004), so the bubbles were in a state of growth when they erupted.

Fig. 6 shows the measured dome velocity profiles and bubble velocity vectors for six different cases and Table 1 charts the results obtained in each experiment. In the first four figures the superficial gas velocity is the same, but the topology of the erupting bubbles is totally different in order to test the validity of the proposed model. For example, the bubble shown in Fig. 6(b) is erupting while another one is coalescing below. At the same time, a different bubble erupts at the surface close to the right side of the first one. From this fact, we can conclude that the particle velocity is higher in the left direction due to the bubble's inability to expand to the right.

The pictures showed in Figs. 6(a), (c), (e) and (f) are examples of the most typical case, in which the velocity profile has a bell shape with the maximum velocity close to the vertical direction at different superficial gas velocities.

The last case, Fig. 6(d), has an atypical velocity profile because the horizontal component is higher than the vertical one, or they have the same order of magnitude. This fact is representative of bubbles demonstrating the *collapsed dome phenomenon*, which usually appears when the center of gravity of the bubble is above the bed surface at the moment of eruption and almost the entire bubble is outside the bed. The bubble is not ingesting the surrounding air, so its velocity is very low in comparison to a bubble of equal size situated at the same height above the distributor, only under the bed surface. In these circumstances, the bubble erupts, but the particles fall from the dome because the vertical component of the ejection velocity is very small. This type of erupting bubbles is similar to those observed by Solimene et al. (2004) and Levy et al. (1982) for isolated erupting bubbles injected into a 3-D fluidized bed.

In almost all the experiments carried out, always the bubble velocity is higher than the growth velocity. Consequently, the maximum particle ejection velocity is equal to the bubble velocity: $\overrightarrow{U}_{p,\max} = \overrightarrow{U}_b$, which is in agreement with the results obtained by Levy et al. (1982) for isolated erupting bubbles.

This maximum particle velocity can be explained by the Davidson model (Davidson and Harrison, 1963). When the bubble nose reaches the bed surface the gas goes through the bubble because the pressure gradient is more favorable. This flow of gas accelerates the particles situated in the nose of the bubble. The gas streamlines in this situation could be similar to the stream lines obtained by Davidson and Harrison (1963) in the slow bubble model.

For the experiments of Fig. 6, we calculated the relative error of the particle ejection velocity, defined as

$$\varepsilon(\theta) = \frac{U_{p,\text{measured}}(\theta) - U_{p,\text{model}}(\theta)}{U_{p,\text{measured}}(\theta)} \tag{10}$$

versus θ, and the results are shown in Fig. 7(a) and (b). The first figure compares ε for the four experiments with the same superficial gas velocity. The relative error for cases (a) and (c)

Table 1
Experimental data of the erupting bubbles showed in Fig. 6

CASE	θ_b (deg)	U_b (cm/s)	U_g (cm/s)	D_{eq} (cm)	U/U_{mf}
(a)	101.3	93.7	25.3	11.4	4
(b)	153.4	41.1	6.2	14.7	4
(c)	99.5	111.8	14.4	14.4	4
(d)	90.0	36.8	10.9	16.6	4
(e)	81.9	93.0	15.8	8.8	3
(f)	76.0	47.7	12.7	11.1	2

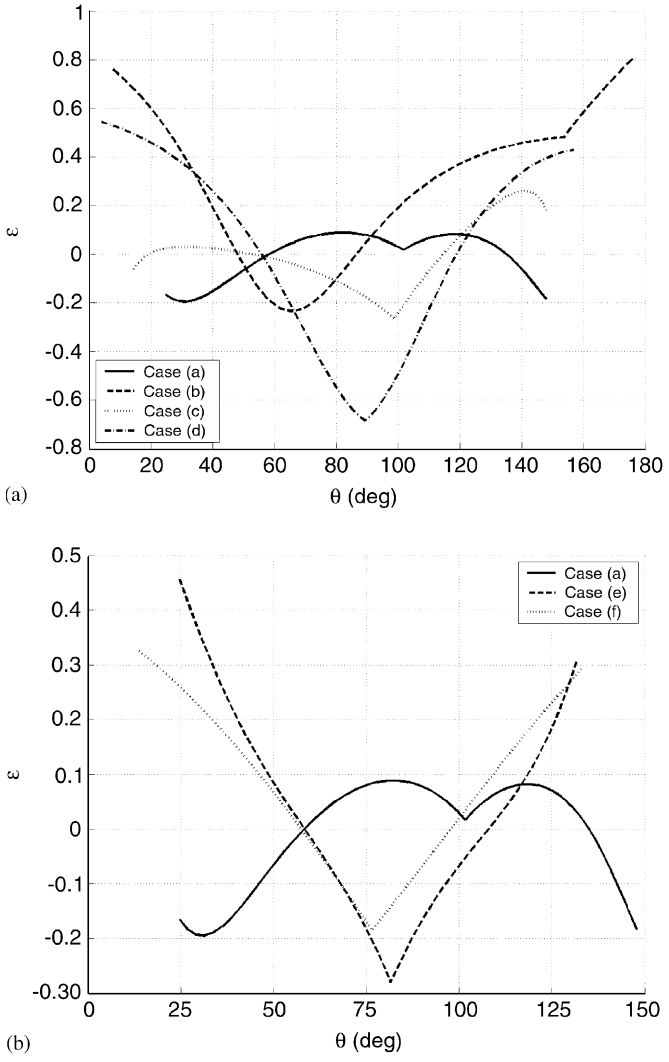

Fig. 7. Relative error versus θ for experiments of Fig. 6. (a) Comparison of four cases with the same superficial gas velocity, and (b) comparison of three cases with different superficial gas velocities.

are under 20% in almost all the angles, which is a very good result. In case (b) the greater error appears at both ends of the profile ($\theta \leqslant 25°$ and $\theta \geqslant 150°$), though in spite of its unusual nature, the error in most of the velocity vectors is under 40%. In the *dome collapsed bubble* (case (d)), the error is maximum in $\theta = 90°$ because this is the direction of the bubble velocity, which does not correspond with the maximum particle velocity direction, as the model supposes. In this case the horizontal

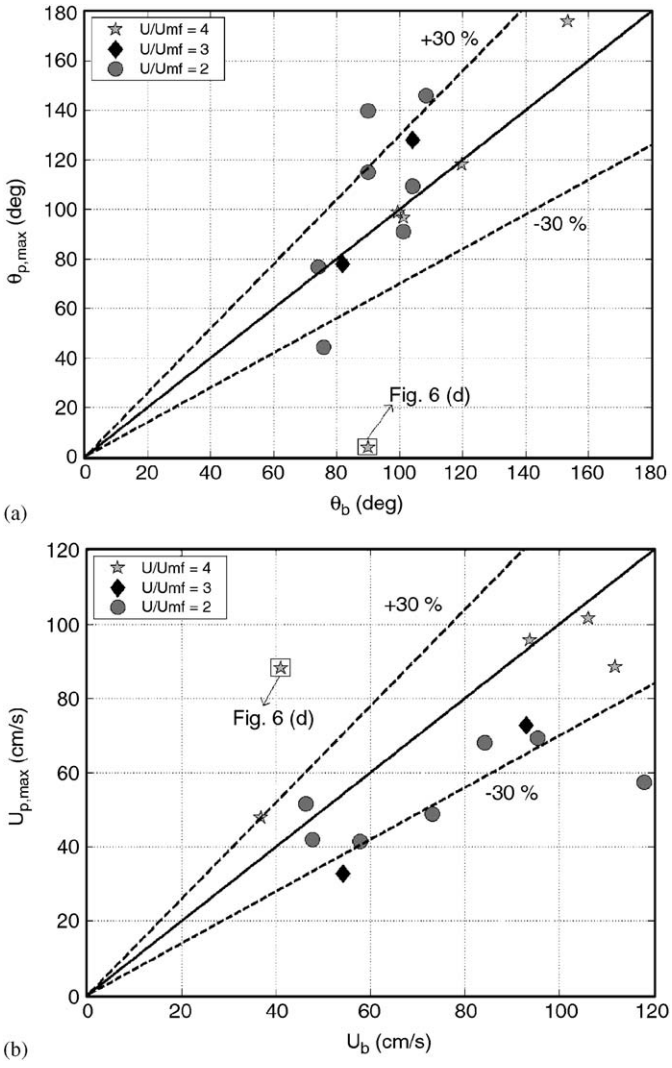

Fig. 8. Comparison of bubble direction (a) and bubble velocity (b) with the direction and velocity of the maximum particle ejection velocity vector measured at different superficial gas velocities. Dashed lines indicate ±30% of error.

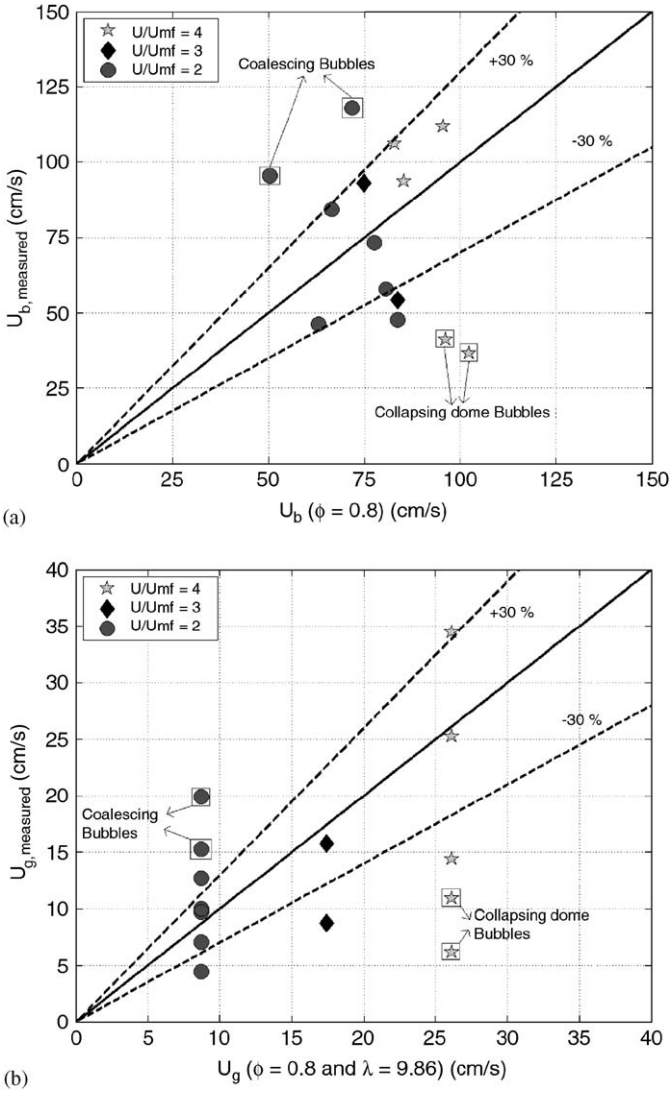

Fig. 9. Comparison of the bubble and growth velocities calculated from Eqs. (7) and (9) with the experimental results (ϕ=0.80 and λ=9.86). Dashed lines indicate ±30% of error.

component of the particle velocity is higher than the vertical component and the model does not correctly estimate the velocity profile. Fig. 7(b) proves the validity of the model with different superficial gas velocities within an accuracy of 30%.

The maximum particle ejection velocity is a very important parameter in the determination of solids entrainment from beds. The presented model, supposes that this maximum particle velocity corresponds in magnitude and direction with the bubble velocity.

Fig. 8(a) compares the direction of the erupting bubble (θ_b) with the angle of the maximum particle velocity vector ($\theta_{p,\max}$) and Fig. 8(b) compares both velocity magnitudes. The results obtained demonstrate that the model effectively predicts the maximum particle velocity in magnitude and direction—except in isolated cases—like the experiment marked with a square, which corresponds with the picture shown in Fig. 6(d). As noted in the previous paragraph, this *collapsed dome*-type eruption is not properly predicted because almost the entire bubble is outside the bed. It is not ingesting surrounding air and the bubble decelerates. Therefore, in this experiment, the maximum particle velocity appears at the stagnation points and not in the direction of the bubble velocity. When the bubble erupts, the particles rain from the dome because the ejection velocity is very low.

Some other researches (Pemberton and Davidson, 1986; Fung and Hamdullahpur, 1993) have estimated the maximum particle velocity for 3-D fluidized beds as $U_{p,\max} \sim 2U_b$. The experiments shown here demonstrate that this supposition overestimates the particle velocity in 2-D fluidized beds. The images in Fig. 6 show that the thickness of the bubble dome layer when the bubble is erupting at the bed surface is $\delta \gg d_p$. This is typical in 2-D beds (Pemberton and Davidson, 1986), while for 3-D beds $\delta \sim d_p$, since the particle flow from the bubble dome is restricted by wall friction.

To obtain an estimation of the bubble and bubble growth velocities, we use a minimum squared technique—a better fit for our results—to calculate the values of ϕ and λ, as can be seen in Eqs. (7) and (9). We obtained a value of $\phi = 0.80$, which concurs with Shen et al. (2004) and $\lambda = 9.86$, higher that the one obtained by Shen et al. (2004). This may be because Eq. (6) is obtained for bubbles growing inside the bed, far removed from the influence of the bed surface. The experiments show that the bubbles grow more slowly when they approach the bed surface, because they ingest less surrounding air. This supposition allows for a higher value of λ.

The results obtained fitting the variables in Eqs. (6) and (7) (λ and ϕ) to the experimental data by minimum square technique are shown in Fig. 9, with two dashed lines indicating a relative error of $\pm 30\%$. Four cases that depart from the global tendency of the bubbles (solid line) are marked with a square. Two of these cases ($U/U_{mf} = 2$) differ from the normal behavior because one bubble is coalescing under the leading one as it erupts at the bed surface. Therefore, its velocity is higher than the velocity of the same bubble without coalesce due to the moment transferred by the coalescing bubble. In the other marked experiments, with $U/U_{mf} = 4$, the *collapsed dome phenomenon* causes the bubble velocity and growth velocity to be lower than we expected.

5. Conclusions

A new model for particle ejection velocity in 2-D fluidized beds is presented, proposing that the particle velocity is the sum of two terms. One of them is related to the bubble velocity and the other to the growth velocity of the bubble. The main conclusions from the present study can be summarized as follows:

(a) A new model for the velocity profile of the particles ejected from the bubble eruptions in 2-D fluidized beds has been presented. This model, unlike those before it, is valid for all bubble shapes and directions, and not only for vertical-ascent circular bubbles.
(b) The model predicts well the velocity profile and takes into account that the velocity of the stagnation points is non-zero. In bubbles that are influenced by the neighboring bubbles (Fig. 6(b)) the result obtained by the model is also acceptable.
(c) The supposition that the maximum particle velocity is equal to $\overrightarrow{U}_b$ produces a favorable result even if θ_b has a value different from the typical $\theta_b \sim 90°$ due to the effect of the other bubbles and the effect of coalescence.
(d) The model does not account as well for *collapsed dome* bubbles, because in these cases the bubble is almost entirely outside of the bed and does not ingest air from the surrounding emulsion phase; hence its velocity is lower than the one proposed by the model. As a result, the horizontal component of the particle velocity is higher than the vertical component, and maximum particle velocity appears at the stagnation points. When this type of bubble bursts at the surface, the particles are not projected to the freeboard; rather, they rain from the dome and return to the bed.
(e) The values of $\overrightarrow{U}_b$ and $\overrightarrow{U}_g$ for bubbles with no coalescence and no collapsed dome can be estimated using Eqs. (7) and (9) with $\phi = 0.8$ and $\lambda = 9.86$.

Notations

A_b	area of the erupting bubble, m^2
A_0	area of distributor per orifice, m^2
b	thickness of the bed, m
d_p	particle diameter, μm
D_{eq}	equivalent diameter, m
g	gravity constant, m/s^2
h	height of bed measured from the distributor, m
R_{eq}	equivalent radius, m
t	time, s
U	superficial gas velocity, m/s
$\overrightarrow{U}_b$	bubble velocity vector, m/s
U_b	magnitude of the bubble velocity vector, m/s
$\overrightarrow{U}_g$	bubble growth velocity vector, m/s
U_g	magnitude of the bubble growth velocity vector, m/s
U_{mf}	minimum fluidization velocity, m/s
$\overrightarrow{U}_p$	particle ejection velocity vector, m/s
U_p	magnitude of the particle ejection velocity vector, m/s
U_p^*	non-dimensional particle ejection velocity, dimensionless
$U_{p,b}$	particle ejection velocity magnitude related to the bubble velocity, m/s
$U_{p,g}$	particle ejection velocity magnitude related to the bubble growth, m/s
$\overrightarrow{U}_{p,max}$	maximum particle ejection velocity vector, m/s
$U_{p,max}$	magnitude of the maximum particle ejection velocity vector, m/s

Greek letters

δ	thickness of the bubble dome layer during bubble eruption, m
ε	relative error, dimensionless
θ	angle formed by the velocity vectors and the bed surface, deg.
θ_b	angle formed by the bubble velocity vector and the bed surface, deg.
θ_{max}	angle formed by the velocity vector at the left stagnation point and the bed surface, deg.
θ_{min}	angle formed by the velocity vector at the right stagnation point and the bed surface, deg.
$\theta_{p,max}$	angle formed by the maximum particle velocity vector and the bed surface, deg.
λ	experimental constant in Eq. (9), dimensionless
ρ_p	particle density, kg/m^3
ϕ	experimental constant in Eqs. (7) and (9), dimensionless

References

Darton, R.C., LaNauze, R.D., Davidson, J.F., Harrison, D., 1977. Bubble growth due to coalescence in fluidised beds. Transactions of the Institute Chemical Engineering 55, 274–280.

Davidson, J.F., Harrison, D., 1963. Fluidized Particles. Cambridge University Press, New York.

Demmich, J., 1984. Mechanism of solid entrainment from fluidized beds. German Chemical Engineering 7, 386–394.

Do, H.T., Grace, J.R., Clift, R., 1972. Particle ejection and entrainment from fluidised beds. Powder Technology 6, 195–200.

Duursma, G.R., Glass, D.H., Rix, S.J.L., Yorquez-Ramírez, M.I., 2001. PIV investigations of flow structures in the fluidised bed freeboard region. Powder Technology 120, 2–11.

Fung, A.S., Hamdullahpur, F., 1993. A gas and particle flow model in the freeboard of a fluidized bed based on bubble coalescence. Powder Technology 74, 121–133.

Geldart, D., 1973. Types of gas fluidization. Powder Technology 7, 285–292.

Glicksman, L.R., Yule, T., 1995. Prediction of the particle flow conditions in the freeboard of a freely bubbling fluidized bed. Chemical Engineering Science 50, 69–79.

Levy, E.K., Dille, J.C., Caram, H.S., 1982. Single bubble eruptions in gas fluidized beds. Powder Technology 32, 173–178.

Pemberton, S.T., Davidson, J.F., 1984. Turbulence in the freeboard of a gas-fluidised beds. The significance of ghost bubbles. Chemical Engineering Science 39 (5), 829–840.

Pemberton, S.T., Davidson, J.F., 1986. Elutriation from fluidized beds—I. Particle ejection from the dense phase into the freeboard. Chemical Engineering Science 41 (2), 243–251.

Peters, M.H., Prybylowski, D.L., 1983. Particle above the surface of a fluidized bed: multiparticle effects. A.I.Ch.E. Symposium Series 79, 83–86.

Santana, D., Nauri, S., Acosta, A., García, N., Macías-Machín, A., 2005. Initial particle velocity spatial distribution from 2-D erupting bubbles in fluidized bed. Powder Technology 150, 1–8.

Shen, L., Johnsson, F., Leckner, B., 2004. Digital image analysis of hydrodynamics two-dimensional bubbling fluidized beds. Chemical Engineering Science 59, 2607–2617.

Solimene, R., Marzocchella, A., Ragucci, R., Salatino, P., 2004. Flow structures and gas-mixing induced by bubble bursting at the surface of an incipiently gas-fluidized bed. Industrial Engineering and Chemical Research 43, 5738–5753.